LA-8630-PR

Progress Report

c.3

Applied Nuclear Data Research and Development

July 1—September 30, 1980

LOS ALAMOS SCIENTIFIC LABORATORY
Post Office Box 1663 Los Alamos, New Mexico 87545

The four most recent reports in this series, unclassified, are LA-8157-PR, LA-8298-PR, LA-8418-PR, and LA-8524-PR.

This report was not edited by the Technical Information staff.

This work was performed under the auspices of the US Department of Energy's Division of Reactor Research and Technology, Office of Basic Energy Sciences, and Office of Fusion Energy; and the Electric Power Research Institute.

UNITED STATES
DEPARTMENT OF ENERGY
CONTRACT W-7405-ENG. 36

LA-8630-PR
Progress Report

UC-34c
Issued: December 1980

Applied Nuclear Data Research and Development

July 1—September 30, 1980

Compiled by

C. I. Baxman
P. G. Young

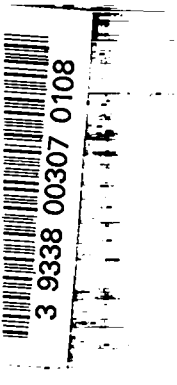

TABLE OF CONTENTS

APPLIED NUCLEAR DATA RESEARCH AND DEVELOPMENT
QUARTERLY PROGRESS REPORT
JULY 1 - SEPTEMBER 30, 1980

Compiled by

C. I. Baxman and P. G. Young

ABSTRACT

This progress report describes the activities of the Los Alamos Nuclear Data Group for the period July 1 through September 30, 1980. The topical content is summarized in The Table of Contents.

I. THEORY AND EVALUATION OF NUCLEAR CROSS SECTIONS

A. Channel Nonorthogonality in R-Matrix Theory (G. M. Hale)

It was described[1] in the last quarterly progress report how channel nonorthogonality at finite radii can induce nonzero overlap (i.e., reduced widths) of cluster-type internal eigenstates with other channel configurations. Possibly an even more important consequence of channel nonorthogonality in light systems is its effect on the relation between the R matrix defined at a finite channel surface and the collision matrix U.

The assumption of channel orthogonality in the usual relation[2] results in surface quantities which are diagonal matrices of S, P, and ϕ; the shift, penetrability, and hard-sphere phase functions, respectively. It appears that the main effect of channel nonorthogonality would be to introduce nonzero off-diagonal elements in these matrices. The nondiagoal elements are complicated integrals that depend on the specific structure of the system under consideration; however, they probably can be evaluated in an approximate and model-dependent manner that would build in some features of direct reaction mechanisms, like particle exchange.

An additional complication is that these effects must be included in such a way that the collision matrix remains unitary, which is equivalent to preserving the hermitian character of the R matrix. Some recent formulations of many-body scattering theory[3,4] that include explicit treatments of channel nonorthogonality could be used, in principle, to construct the required R matrix. It is not yet known whether these theories lead to a practically calculable procedure, but the possibility is being pursued.

B. Evaluation of the Ga(n,γ) Reaction (P. G. Young)

In a recent progress report,[1] an updated n + Ga evaluation that was submitted for Revision 1 of ENDF/B-V is described. As a result of Phase I review comments (D. Larson, ORNL), the Ga(n,γ) cross section was modified to better agree with experimental data. In particular, minor revisions were made in the evaluation from 0.8 to 4 keV to improve agreement with Konks' data[2] (see Fig. 1), and more extensive changes based on Dovbenko's[3] and Zaikin's[4] data were made between 20 keV and 5 MeV (see Fig. 2). The revised evaluation has been approved for ENDF/B-V.1 and has been issued by the National Nuclear Data Center at Brookhaven.

C. New Calculations of Neutron-Induced Cross Sections on Tungsten Isotopes [E. D. Arthur and C. A. Philis (Bruyeres-le-Chatel)]

Nuclear model calculations have been completed for $^{182,183,184,186}W$ isotopes in the energy range from 0.001 to 20 MeV. These results form the basis of a new tungsten evaluation[9] that should correct energy balance and neutron emission spectra problems occurring in the present ENDF/B-V evaluation.

Cross sections were calculated with the ECIS78,[10] COMNUC,[11] and GNASH[12] nuclear model codes. The ECIS78 code was used to determine cross sections for neutron inelastic scattering from the 2^+ and 4^+ states in $^{182,184,186}W$ and the $3/2^-$, $5/2^-$, $7/2^-$, and $9/2^-$ states in ^{183}W. In addition, this code was also used to provide shape elastic scattering cross-section results as well as to provide deformed optical model neutron transmission coefficients for use in the COMNUC and GNASH codes. The Hauser-Feshbach statistical model code COMNUC was used between 0.001 and 6 MeV to provide capture, compound elastic, and compound inelastic cross sections (both to discrete levels and to the continuum) since it includes width-fluctuation corrections. Above 6 MeV the GNASH code was used since it handles multistep reaction chains and also includes

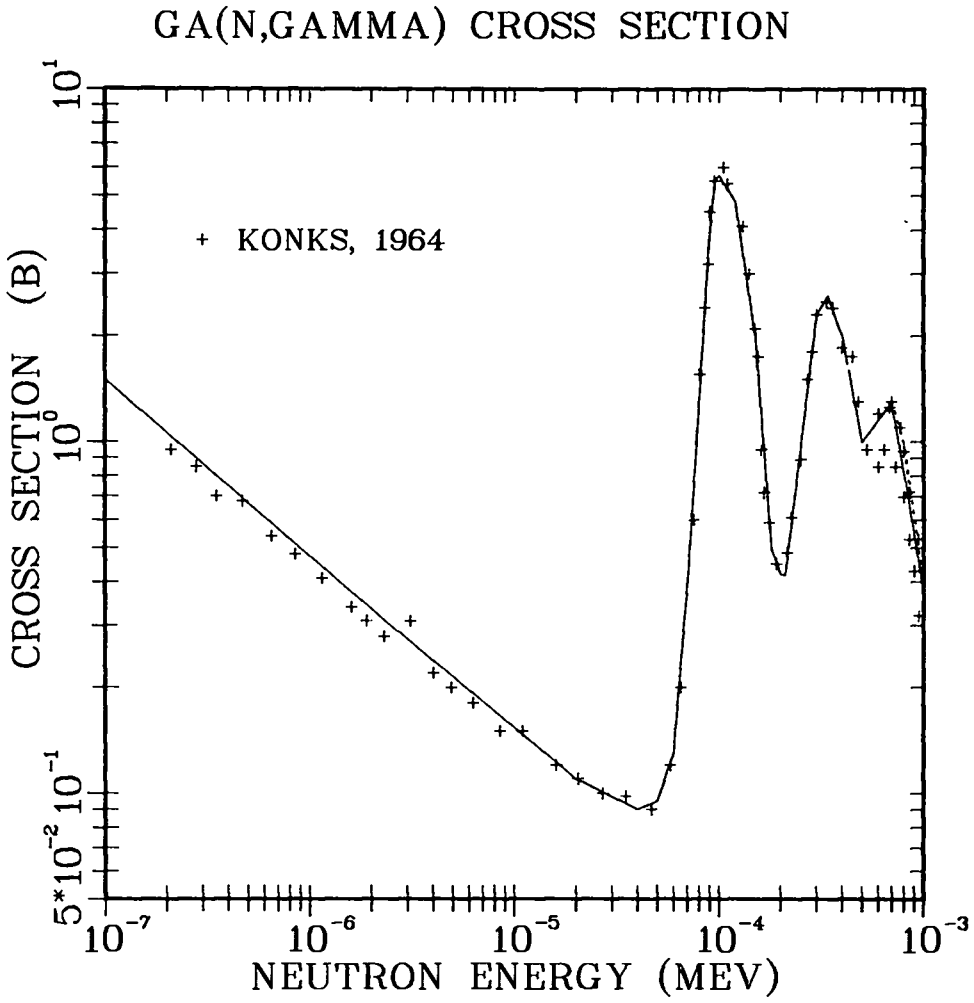

Fig. 1.
The Ga(n,γ) cross section from 0.1 eV to 10 keV. The solid curve is the present evaluation and the dashed curve is ENDL-78.

preequilibrium corrections important for cross-section and spectral results above 10 MeV.

Input parameters were determined in a manner similar to our previous efforts;[13,14] that is, independent data types were used to arrive at a consistent set of needed parameters. Gamma-ray strength functions (f_{E1}) were determined from analyses of $^{182,183,184,186}W(n,\gamma)$ data and are generally consistent with

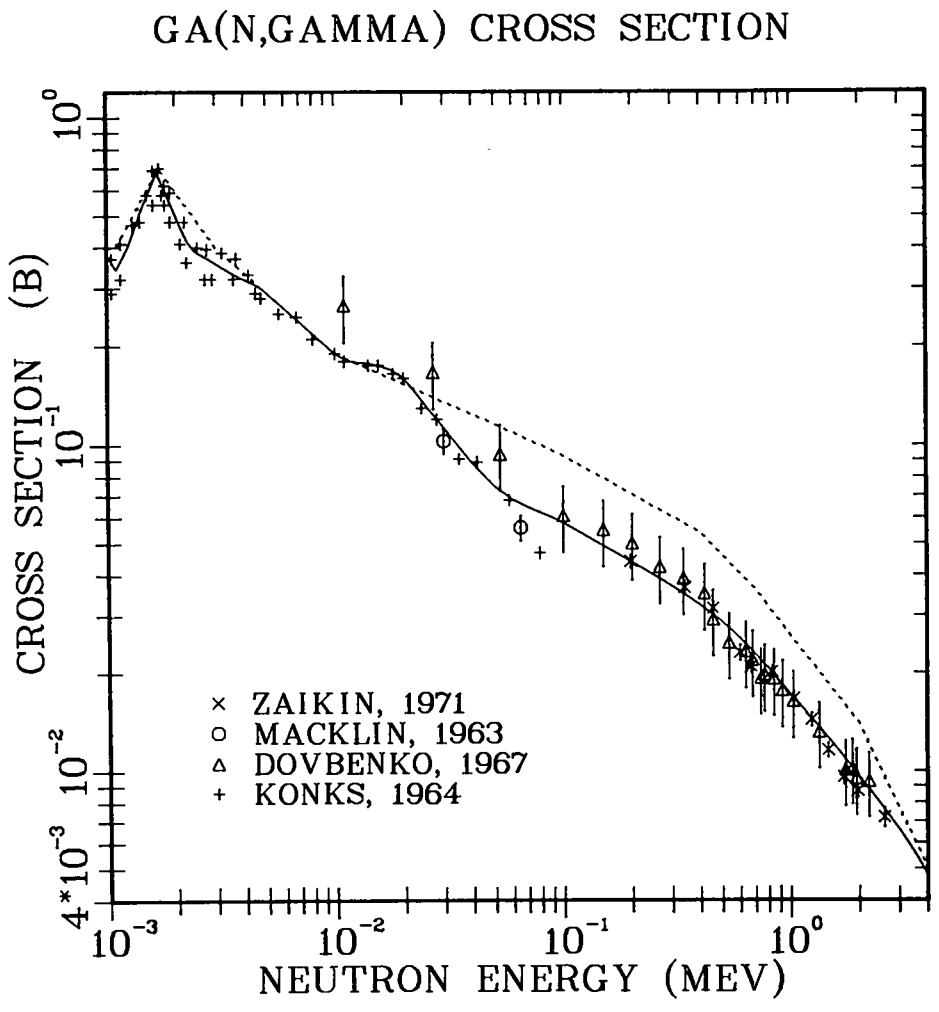

Fig. 2.
The Ga(n,γ) cross section from 1 keV to 4 MeV. The solid curve is the present evaluation and the dashed curve is ENDL-78.

the experimentally determined f_{E1} values of Joly.[15] The maximum amount of discrete level information was used throughout the calculations since cross sections resulting from transitions to discrete levels can be important, particularly around the (n,2n) threshold. The level density expressions of Gilbert and Cameron[16] were used to represent the continuum excitation energy regions after adjustment of parameters to fit discrete level and s-wave resonance spacing information.

Recently Delaroche[17] determined optical model parameters from coupled channel analyses of neutron data on $^{182,183,184,186}W$, which we hoped to use in our calculations. Data in his analyses included neutron total cross sections from 0.1 to 15 MeV, elastic scattering angular distributions up to 4 MeV (but primarily at 3.4 MeV where new measurements have been made at Bruyeres-le-Chatel), and inelastic scattering angular distributions for 2^+ and 4^+ states (again primarily at 3.4 MeV). In addition, 16 MeV (p,p') data on $^{182,184,186}W$ were used and overall a good fit was obtained to these various data types. We applied these parameters to generate coupled-channel transmission coefficients to use in GNASH calculations of the $^{184}W(n,2n)$ cross section. We used the gamma-ray strength functions determined previously and found we were unable to achieve good agreement with new measurements of this cross section by Frehaut[18] from threshold to 15 MeV. Our calculations overestimated the experimental data by 20-40% around threshold, and at higher energies (12-14 MeV) there was a consistent 8-10% overestimation of the cross section.

For calculations of the $^{186}W(n,2n)$ cross section, the overpredictions were worse (25-200%) around threshold (E_n = 8-10 MeV). Part of the reason for this worsening situation is shown in Fig. 3 where cross sections for direct population of levels in the ^{183}W and ^{185}W residual nuclei [by the ^{184}W and $^{186}W(n,2n)$ reactions, respectively] are shown for calculations performed at the same energy above the (n,2n) threshold (U_R = 1.75 MeV) using the Delaroche parameters. Evident is the preferred population of positive parity states having high spins due in part to the initial spin distributions (centered around J = 5) calculated for the compound nucleus formation cross section at these incident energies ($\sim$9 MeV). In ^{185}W, the density of high spin states within the excitation energy region up to 0.8 MeV is greater than for ^{183}W and such states lie at slightly lower excitation energies so that the energy of the transition is greater. Thus under similar conditions, the theoretical $^{186}W(n,2n)$ cross section lies about 20% higher than that for ^{184}W, whereas the experimental results show no such effect. Spins and parities for these levels are well known and attempts to improve the agreement by adjustment of the gamma-ray competition lead to unphysical values for the gamma-ray strength function. We thus felt it was necessary to modify the Delaroche optical parameter values to provide better agreement with these data.

To adjust these parameters, we included the same data as was used in the Delaroche parameter determinations [neutron total, elastic, and inelastic

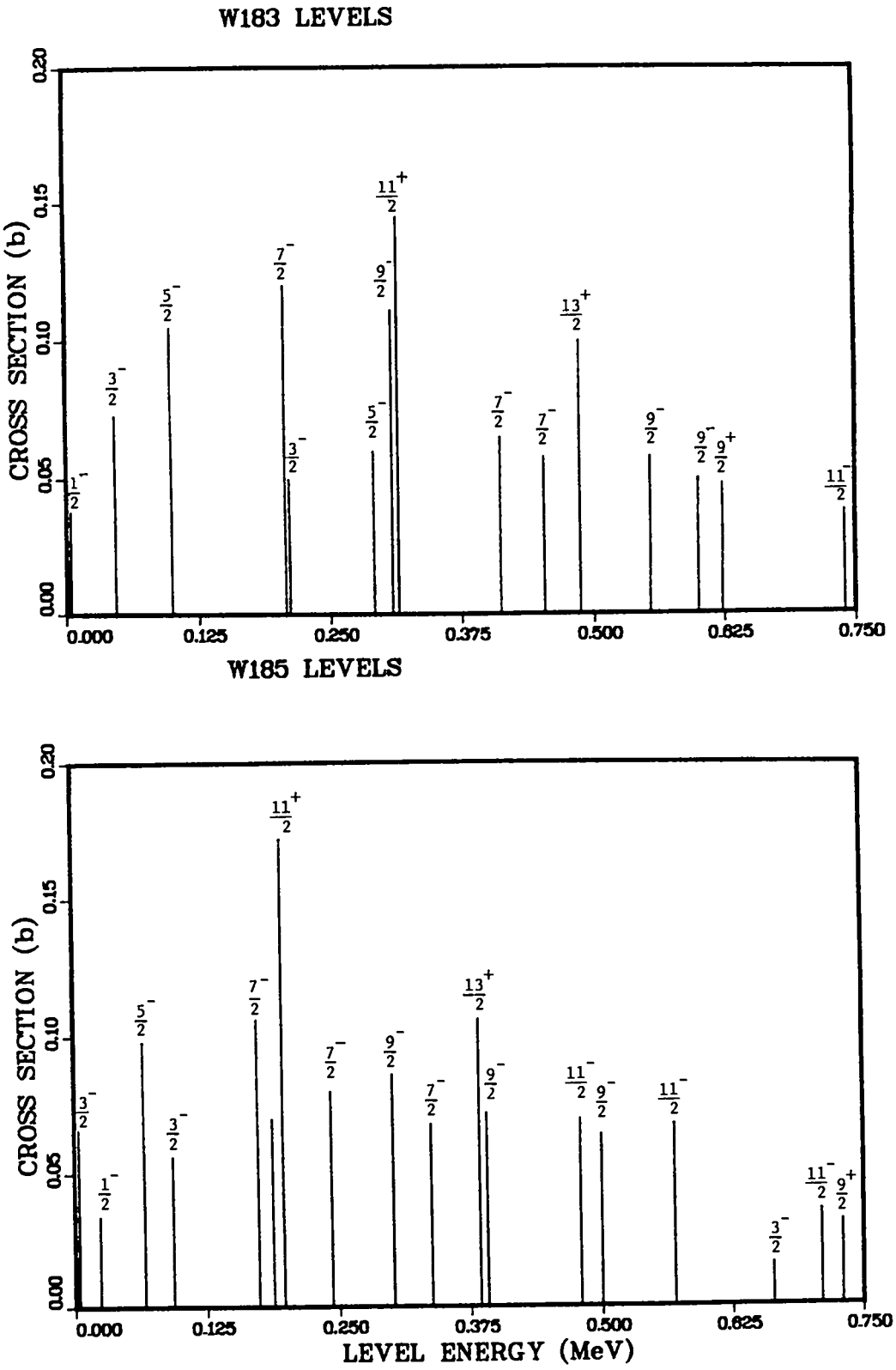

Fig. 3.
Production of discrete levels in the ^{183}W and ^{185}W residual nuclei from $^{184,186}W(n,2n)$ reactions calculated 1.75 MeV above threshold using the Delaroche optical parameters.

angular distributions and 16 MeV (p,p') data] with the added, indirect constraint of the Frehaut (n,2n) cross-section measurements. The resulting optical parameters appear in Table I. They are similar in form to the Delaroche set but generally involve small adjustments in the geometrical parameters for the real and imaginary well depths. The form of the energy dependence of the surface derivative imaginary well depth was changed to include a linear dependence on energy (instead of $\sqrt{E}$). Also, the energy at which a transition in the form of the surface imaginary well depth occurred was altered. For the ^{186}W calculations, the β_2 value was decreased from the Delaroche result of 0.203 ± 0.006 to 0.195. These parameter changes did not significantly alter the agreement obtained to the neutron total, differential elastic and inelastic data, and to the (p,p') results described above. An improvement in the calculated (n,2n) cross section did occur as shown for ^{184}W(n,2n) in Fig. 4, where the solid curve is the results obtained using the parameters of Table I and the dashed curve the results from use of the Delaroche parameter set.

Further tests of these calculated results were made to excitation functions for elastic and inelastic scattering up to 4 MeV measured by Guenther et al.[19] and to experimental results for gamma-ray and neutron emission spectra. Figure 5 compares our calculated gamma-ray production spectrum induced by 13-MeV neutrons to the data of Dickens.[20] In Fig. 6 our neutron emission spectrum calculated for 14.6 MeV neutron interactions with ^{184}W is compared to the Hermsdorf[21] measurements for natural tungsten. The dashed curve shows results from the ENDF/B-V evaluation.

Results from these calculations (neutron and gamma-ray cross sections and spectra) are presently being assembled in an ENDF format to produce individual evaluations for the four tungsten isotopes.

D. Calculation of Prompt Fission Neutron Spectra and $\bar{\nu}_p$ [D. G. Madland and J. R. Nix (T-9)]

An extensive journal article summarizing this work is near completion. Our most recent communcation[22] presents recommendations on the evaluation of prompt fission neutron spectra and $\bar{\nu}_p$ in the light of the theoretical work summarized in this article.

Documentation of the FISPEK code is continuing.

TABLE I

OPTICAL PARAMETERS FOR TUNGSTEN ISOTOPES*

	r	a
^{182}W		
$V = 46.8 - 0.4E$	1.26	0.61
$W_{vol} = -1.8 + 0.2E$	1.26	0.61
$V_{SO} = 7.5$	1.26	0.61
$W_{SD} = 3.68 + 0.76E$	1.24	0.45
Above 4.75 MeV		
$W_{SD} = 7.29 - 0.1E$		
$\beta_2 = 0.223$, $\beta_4 = -0.054$		
^{183}W		
$V = 46.7 - 0.4E$	1.26	0.61
$W_{vol} = -1.8 + 0.2E$	1.26	0.61
$V_{SO} = 7.5$	1.26	0.61
$W_{SD} = 3.54 + 0.76E$	1.24	0.45
Above 4.63 MeV		
$W_{SD} = 7.055 - 0.1E$		
$\beta_2 = 0.22$, $\beta_4 = -0.055$		
^{184}W		
$V = 46.6 - 0.4E$	1.26	0.61
$W_{vol} = -1.8 + 0.2E$	1.26	0.61
$V_{SO} = 7.5$	1.26	0.61
$W_{SD} = 3.4 + 0.76E$	1.24	0.45
Above 4.5 MeV		
$W_{SD} = 6.82 - 0.1E$		
$\beta_2 = 0.209$, $\beta_4 = -0.056$		
^{186}W		
$V = 46.6 - 0.4E$	1.26	0.61
$W_{vol} = -1.8 + 0.2$	1.26	0.61
$V_{SO} = 7.5$	1.26	0.61
$W_{SD} = 3.12 + 0.76E$	1.24	0.45
Above 4.25 MeV		
$W_{SD} = 6.35 - 0.1E$		
$\beta_2 = 0.195$, $\beta_4 = -0.057$		

*All well depths are in MeV, geometrical parameters are in fm.

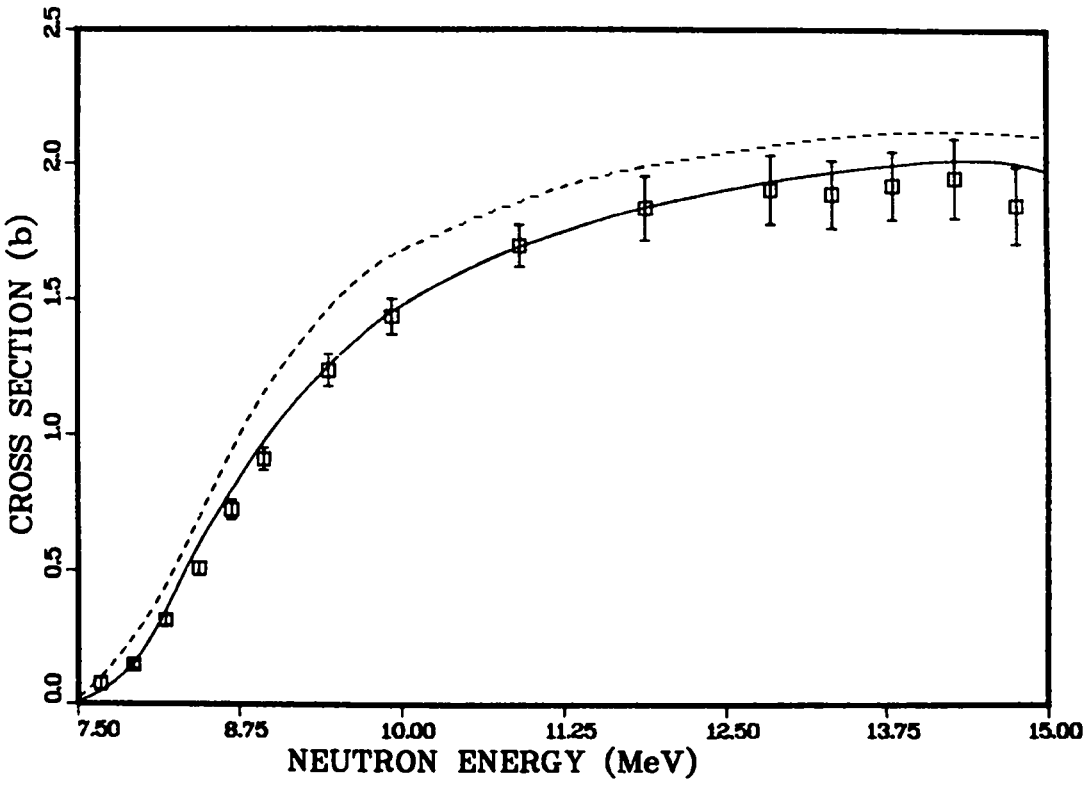

Fig. 4.
Calculated values of the $^{184}W(n,2n)$ cross section using the parameters of Table I (solid curve) are compared to the Frehaut data. The dashed curve indicates results obtained with the Delaroche parameters.

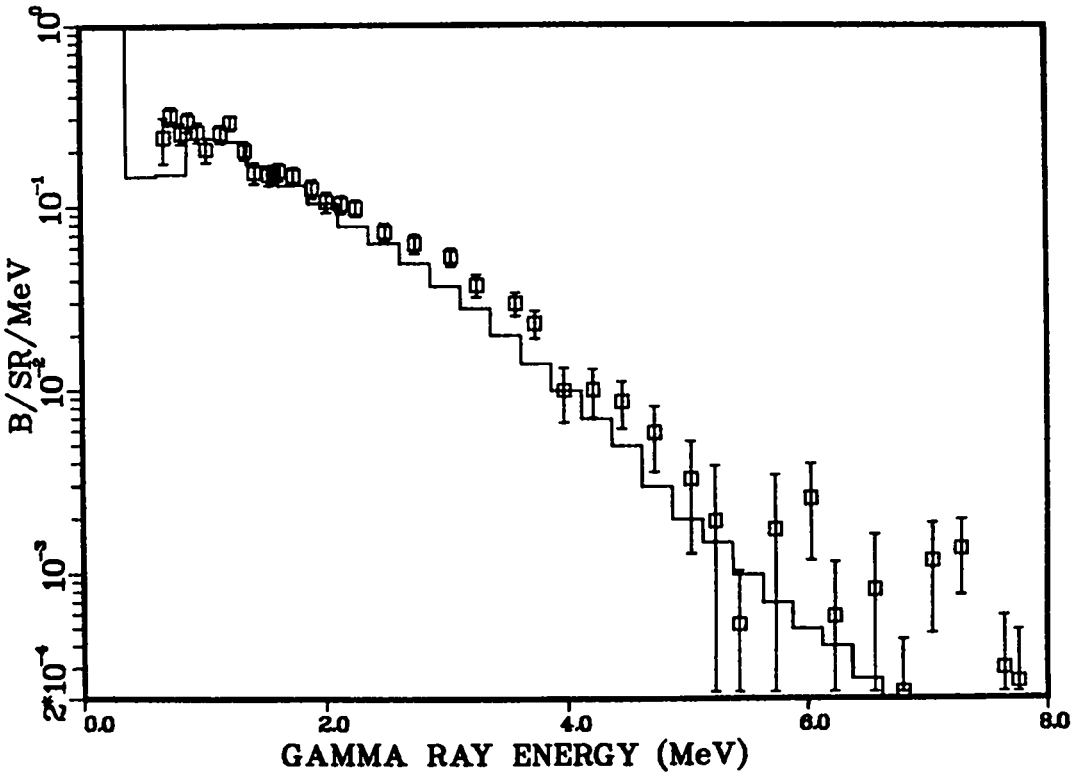

Fig. 5.
Calculated and experimental gamma-ray production spectra from 13 MeV neutron interactions with tungsten.

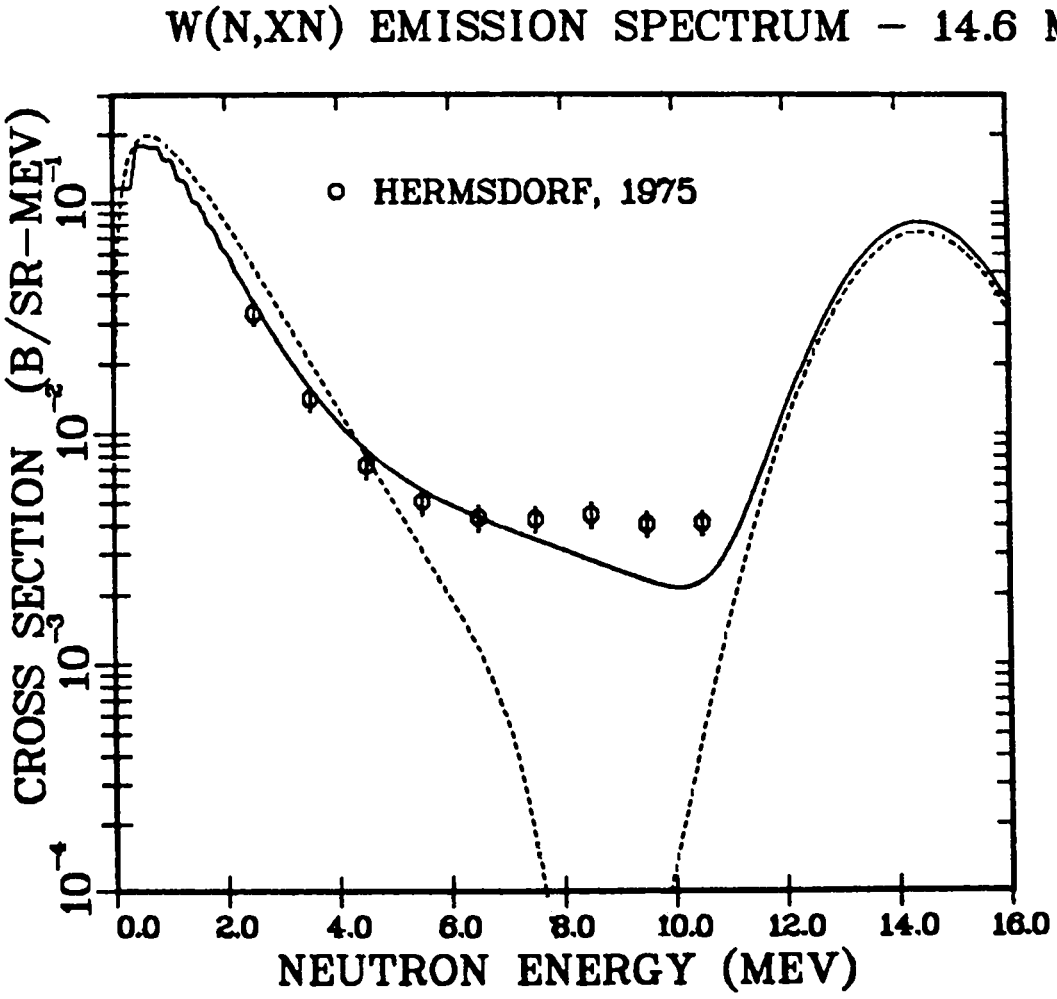

Fig. 6.
Calculated neutron emission spectra induced by 14.6 MeV neutrons on ^{184}W are compared to the Hermsdorf measurements on natural tungsten. The dashed curve represents results from the ENDF/B-V evaluation.

E. Calculation of Prompt Fission Neutron Spectra and $\bar{\nu}_p$ for the Neutron-Induced Fission of ^{239}U and ^{240}U (D. G. Madland, R. M. Boicourt, and R. E. MacFarlane)

The prompt fission neutron spectrum N(E) and the average prompt neutron multiplicity $\bar{\nu}_p$ have been calculated for the neutron-induced fission of ^{239}U and ^{240}U. The results have been inserted into the local LASL evaluations of ^{239}U and ^{240}U, which are used in the X-Division continuous-energy Monte-Carlo library. The evaluations are available on the Los Alamos common file system (CFS) path

/ENDF/5/A/T/102 .

In the interest of a simple and fast representation for N(E), the energy-dependent Watt distribution was used in approximation to the exact spectrum.[23,24] In the ENDF notation, the energy-dependent Watt distribution is the LF=11 law under MF=5, with energy-dependent parameters $A(E_n)$ and $B(E_n)$ where E_n is the kinetic energy of the neutron inducing fission. Using the ENDF notation our results are as follows.

$^{239}U + n(E_n)$

$$A(\text{Watt}) = \frac{8}{9}\left[\frac{21.196 + E_n(\text{MeV})}{24.0}\right]^{1/2} \quad \text{MeV}.$$

$$B(\text{Watt}) = \frac{81}{16}\left[\frac{18.163}{21.196 + E_n(\text{MeV})}\right] \quad \text{MeV}^{-1}.$$

$^{240}U + n(E_n)$

$$A(\text{Watt}) = \frac{8}{9}\left[\frac{19.842 + E_n(\text{MeV})}{24.1}\right]^{1/2} \quad \text{MeV}.$$

$$B(\text{Watt}) = \frac{81}{16}\left[\frac{18.182}{19.842 + E_n(\text{MeV})}\right] \quad \text{MeV}^{-1}.$$

The average prompt neutron multiplicity $\bar{\nu}_p$ was calculated as a function of the incident neutron energy E_n using the "Simulated Energy-Dependence of

$\sigma_c(\varepsilon)$" approach discussed in the journal article we are planning to publish. The total average prompt gamma-ray energy per fission is required as input to this calculation and, in the case of ^{239}U and ^{240}U, was obtained from the work of Hoffman and Hoffman.[25] Our results are as follows.

$^{239}U + n(E_n)$

$$\bar{\nu}_p(E_n) = \frac{14.386 + E_n(\text{MeV})}{4.893 + [4T_m(\text{MeV})/3]} \quad , \text{where}$$

$$T_m = \left[\frac{21.196 + E_n(\text{MeV})}{24.0}\right]^{1/2} \quad \text{MeV}.$$

$^{240}U + n(E_n)$

$$\bar{\nu}_p(E_n) = \frac{13.004 + E_n(\text{MeV})}{4.839 + [4T_m(\text{MeV})/3]} \quad , \text{where}$$

$$T_m = \left[\frac{19.842 + E_n(\text{MeV})}{24.1}\right]^{1/2} \quad \text{MeV}.$$

F. Calculation of Prompt Fission Neutron Spectra for $^{242}Cm(sf)$ and $^{244}Cm(sf)$ (D. G. Madland)

At the request of LASL group Q-5, the prompt fission neutron spectrum N(E) has been calculated for the spontaneous fission of ^{242}Cm and ^{244}Cm. The calculations have been performed for emitted neutron energies E ranging from 0.1 keV to 20.0 MeV. The physical units used are E (MeV) and N(E) (MeV^{-1}). The theoretical spectrum is defined such that

$$\int_0^\infty N(E)dE = 1 \quad .$$

The results have been stored on the Los Alamos CFS in the green file CMQ5 using E,N(E) pairs in FORMAT(5X,2(1PE15.6)). The first 461 pairs are for ^{242}Cm(sf) while the second 461 pairs are for ^{244}Cm(sf). The file CMQ5 can be accessed using the command

```
MASS GET DIR=/081380/WCODES CMQ5    .
```

The theoretical work upon which these calculations are based in described in Refs. 22-24. The present calculations were performed using the "Simulated Energy-Dependence of $\sigma_c(\varepsilon)$" approach to be discussed in our next publication. While little or no experimental prompt fission neutron spectra data exist for ^{242}Cm(sf) and ^{244}Cm(sf), experimental data do exist for the average prompt neutron multiplicity $\bar{\nu}_p$ for these cases. Since the formalism that we use to calculate N(E) is also used to calculate $\bar{\nu}_p$, a test of the N(E) calculation is made by comparing calculated and measured $\bar{\nu}_p$ values. For the present calculation, the results are

^{242}Cm(sf): $\bar{\nu}_p$ (exp) = 2.51 $\pm$ 0.06

$\bar{\nu}_p$ (calc) = 2.488

Relative Difference = 0.88% ,

^{244}Cm(sf): $\bar{\nu}_p$ (exp) = 2.681 $\pm$ 0.011

$\bar{\nu}_p$ (calc) = 2.660

Relative Difference = 0.78% ,

where the experimental data are from Ref. 26. Because the $\bar{\nu}_p$ calculation relies heavily upon energy balance in the fission process, the excellent agreement between experiment and theory indicates that the correct energy dissipation was used in calculating N(E). This, in turn, means that the slope of the tail of N(E) is correctly calculated.

II. NUCLEAR CROSS SECTION PROCESSING

A. ENDF/B-V Processing (R. B. Kidman)

The multigroup data of the 93-isotope 70-group ENDF/B-V library has been reprocessed this quarter. The new library now additionally contains P_5 cross sections and elastic removal f-factors for every isotope plus fission source matrices for all isotopes that have a fission cross section. The transport f-factors have also been redefined.

$$f^g_{tr}(\text{previously}) = \frac{\sigma^g_{t,1}(T,\sigma) - \mu^g \sigma^g_{e,0}(T,\sigma)}{\sigma^g_{t,1}(0,\infty) - \mu^g \sigma^g_{e,0}(0,\infty)}$$

$$f^g_{tr}(\text{currently}) = \frac{\sigma^g_{t,1}(T,\sigma) - \sum_{g'} \sigma^{g\to g'}_{s,1}(T,\sigma)}{\sigma^g_{t,1}(0,\infty) - \sum_{g} \sigma^{g\to g'}_{s,1}(0,\infty)}$$

B. THOR Calculations (R. B. Kidman)

Last quarter, the relatively high computed eigenvalues for the small reflected assemblies BIGTEN, FLATTOP-25, FLATTOP-PU, FLATTOP-23, and THOR were thought to be a result of using only P_3 cross sections. Modifications were made to data preparation and transport codes so that the new P_5 cross sections could be tested on the THOR assembly. The eigenvalue results are

ORDER	EIGENVALUE
P_0	1.1514
P_1	0.9917
P_2	1.0265
P_3	1.0152
P_4	1.0189
P_5	1.0178

Obviously the P_5 eigenvalue (or any higher order eigenvalue) will not solve the high eigenvalue problem of the THOR assembly. This eliminates one speculation for the cause of the high eigenvalues of the small reflected assemblies. Speculation now centers on the previous fission source treatment. This speculation will be tested when the codes are modified to handle the new fission source matrices.

When the THOR eigenvalues are plotted versus Legendre order, the asymptotic behavior becomes apparent. It appears that the even order eigenvalues approach the P_∞ eigenvalue from above while the odd order eigenvalues approach it from below. Therefore, even order eigenvalues are always high while odd order eigenvalues are always low. The asymptotic approaches to the P_∞ eigenvalue also appear to be smooth and monotonic. In view of this behavior, it would seem to be a simple and useful modification to have physics codes compute and print out an accurate estimate of the P_∞ eigenvalue based on their current P_i calculations.

C. Thermal Reactor Code Comparisons (R. E. MacFarlane)

A powerful technique for verifying thermal power reactor analysis codes such as EPRI-CELL and EPRI-CPM is to compare them with a continuous-energy Monte-Carlo code. Such comparisons are most meaningful if simplified problems are used that focus on selected aspects of the calculation. Several "numerical benchmarks" of this kind have been specified by the Electric Power Research Institute (EPRI).[22] The numerical benchmarks are also very useful for comparing different versions of a code run at different installations. As reported last quarter, this type of comparison was used to remove some differences between the LASL and EPRI versions of EPRI-CELL.

Numerical benchmark #5 (BENCH5) was chosen to test the range of high fuel-to-moderator volume ratios characteristic of Boiling Water Reactors (BWR). Specifications are given in Table II.

The first results from BENCH5 showed some serious disagreements that have been traced to an inconsistency between the CELL and CPM treatments of resonance interference. The error was found to be in CELL; the theory used was experessed in terms of a group resonance integral even though the code actually required a group cross section.

In addition to this fix, the resonance input and method of computing the epithermal disadvantage coefficient were changed. The standard version required a calculation of Dancoff corrections outside the code, and it also had some of the cross sections used in computing resonance self-shielding corrections given in the code in DATA statements. The new version makes these calculations after the cross-section libraries have been read so that all parameters used are consistent. It is no longer necessary to construct the RES array for general

TABLE II

SPECIFICATIONS FOR EPRI NUMERICAL BENCHMARK #5

Temperature (all regions) 300 K

Fuel region

outside radius	0.4675 cm
^{235}U density	0.694117-3
^{238}U density	0.218195-1
^{16}O density	0.450473-1

Clad region

outside radius	0.5290 cm
^{27}Al density	0.473054-1

Moderator region

hexagonal lattice pitch	1.1660 cm
equiv. cylinder radius	0.6122 cm
^{1}H density	0.667804-1
^{16}O density	0.333902-1

Required results

k_∞

4-group cell-averaged cross sections

4-group cell fluxes

energy bounds

10	Mev
821	keV
5.53	keV
0.625	eV
1.-5	eV

input. These changes simplify the input and reduce the possibility of user errors.

The BENCH5 results for four codes are compared in Table III. A careful look at the reaction rates shows that much of the difference between CELL and CPM comes from the difference in ^{235}U fission in group 3. This may result from the difficulty CPM has in representing resonance interference using its comparatively coarse group structure. To be more specific, ^{235}U has an important pair of resonances just below 10 eV. CPM thinks that they overlap with the 6.7 eV ^{238}U resonance because they are all in the 4-10 eV group, but CELL knows that there is no overlap by virtue of its smaller groups. Most of the other differences are smaller and close to the statistical uncertainty in the Monte-Carlo results. It should be noted that the MCNP calculation used a white cylindrical boundary while the SAM-CE results are based on a hexagonal cell--this may explain some of the difference in multiplication.

D. Covariance Plotting Capability (D. W. Muir)

A computer program CPL has been written to read a multigroup covariance matrix in the format produced by the ERRORR module of NJOY,[28] convert it to the form of two separate relative-standard-deviation vectors and a correlation matrix, and then plot the vectors and matrix side-by-side. The plotting is accomplished with the aid of the proprietary plotting software package DISSPLA.[29] Examples of the types of plot produced by CPL are shown in Figs. 7-9. The plots were generated from multigroup covariance matrices for the two reactions $^{10}B(n,\alpha_0)^7Li$(g.s.) and $^{10}B(n,\alpha_1)^7Li$(0.48 MeV), which in turn were produced from the ENDF/B-V evaluation for ^{10}B (MAT 1305) using ERRORR. The group structure chosen in ERRORR was identical to the energy grid used in the evaluation except that the structure was truncated at 40 keV at the lower end and 1 MeV at the upper end. Thus, the plotted data are essentially identical to the evaluated covariances for the reactions shown. When used in this mode, the combination of ERRORR and CPL may provide a useful tool for validating ENDF/B uncertainty evaluations. CPL will be incorporated into a new NJOY module that will perform a variety of covariance output formatting and plotting tasks.

TABLE III

THERMAL REACTOR CODE COMPARISONS FOR BENCH5

Parameter	EPRI-CELL	EPRI-CPM	MCNP	SAM-CE
k_∞	1.1332	1.1251	1.1337	1.1400
$^{235}U(n,f)$[a]	1.236	1.242	1.239	1.244
	1.634	1.637	1.639	1.644
	21.80	21.15	22.05	21.71
	247.9	245.6	244.2	242.8
$^{235}U(n,\gamma)$	0.0650	0.0654[b]	0.0649	0.0650
	0.4669	0.4671	0.4663	0.4695
	10.87	11.17	10.61	10.58
	44.39	43.97	43.77	43.49
$^{238}U(n,f)$	0.3622	0.3646	0.3626	--
$^{238}U(n,\gamma)$	0.0583	0.0584[b]	0.0581	0.0582
	0.2494	0.2512	0.2625[c]	0.2461
	1.654	1.646	1.660	1.647
	1.290	1.280	1.274	1.263

[a]Four-group cell-averaged values.

[b]Corrected using CELL (n,2n) cross section.

[c]No unresolved self-shielding.

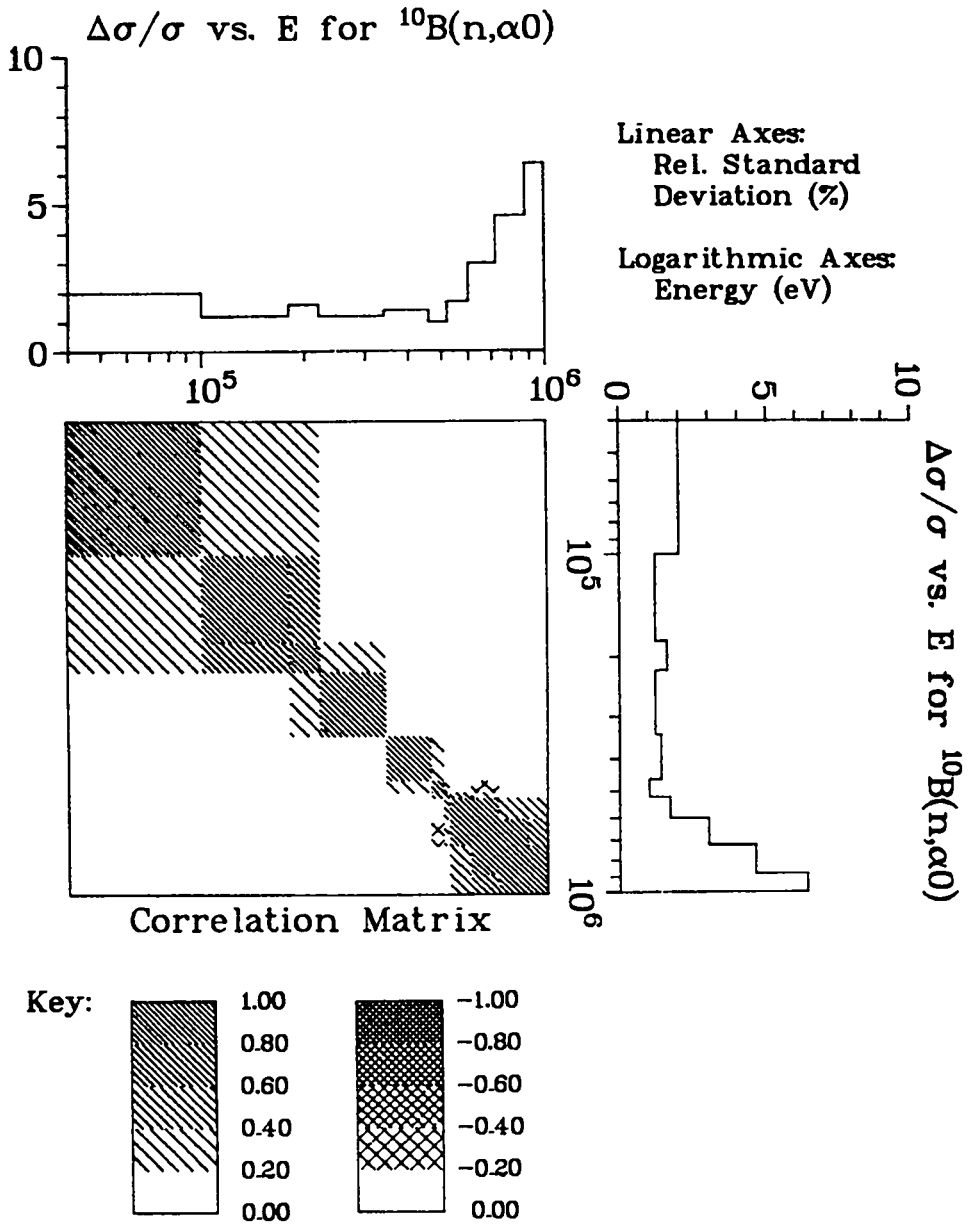

Fig. 7.
Covariances for (MAT 1305, MT 780).

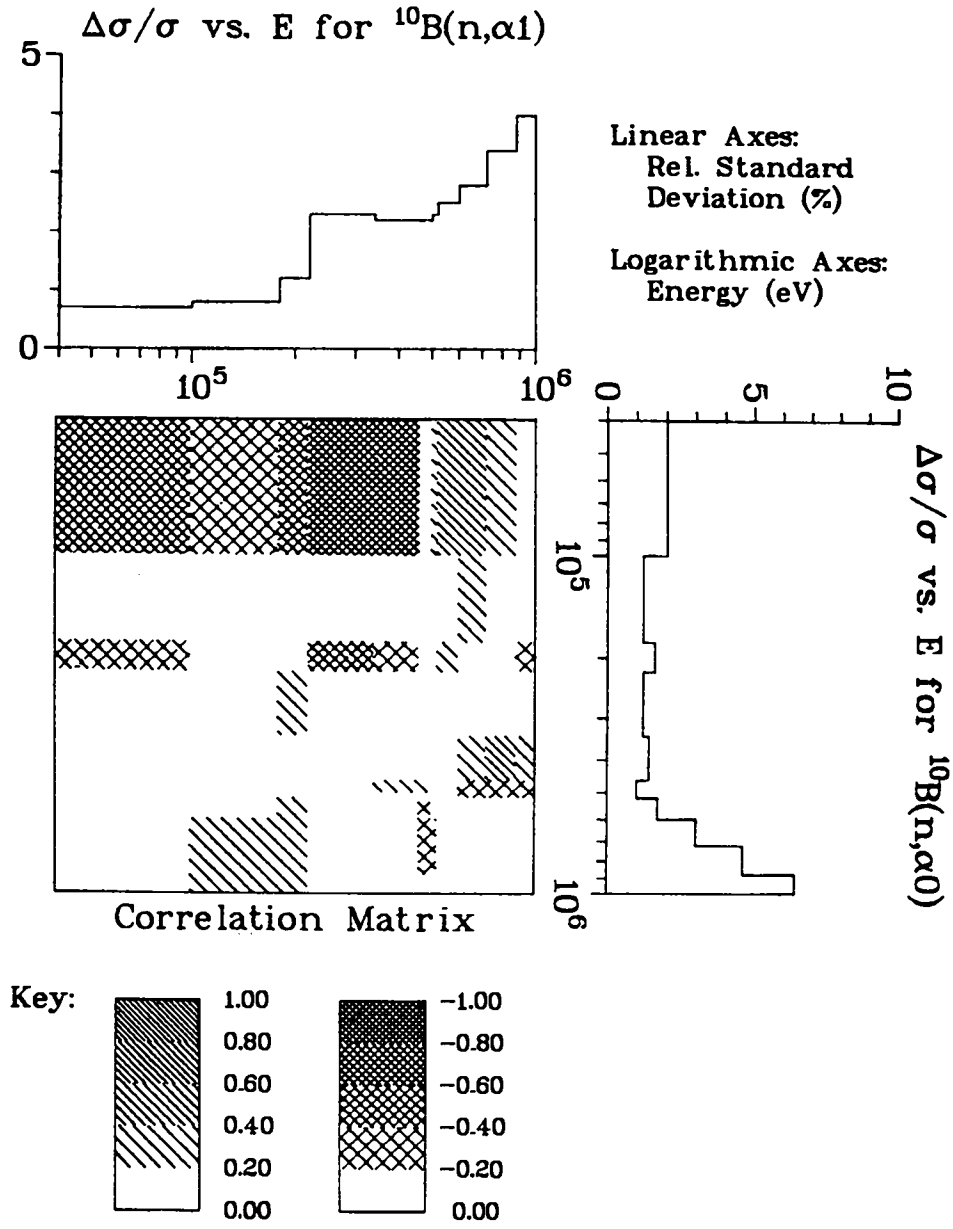

Fig. 8.
Covariances for (MAT 1305, MT 780) with (MAT 1305, MT 781).

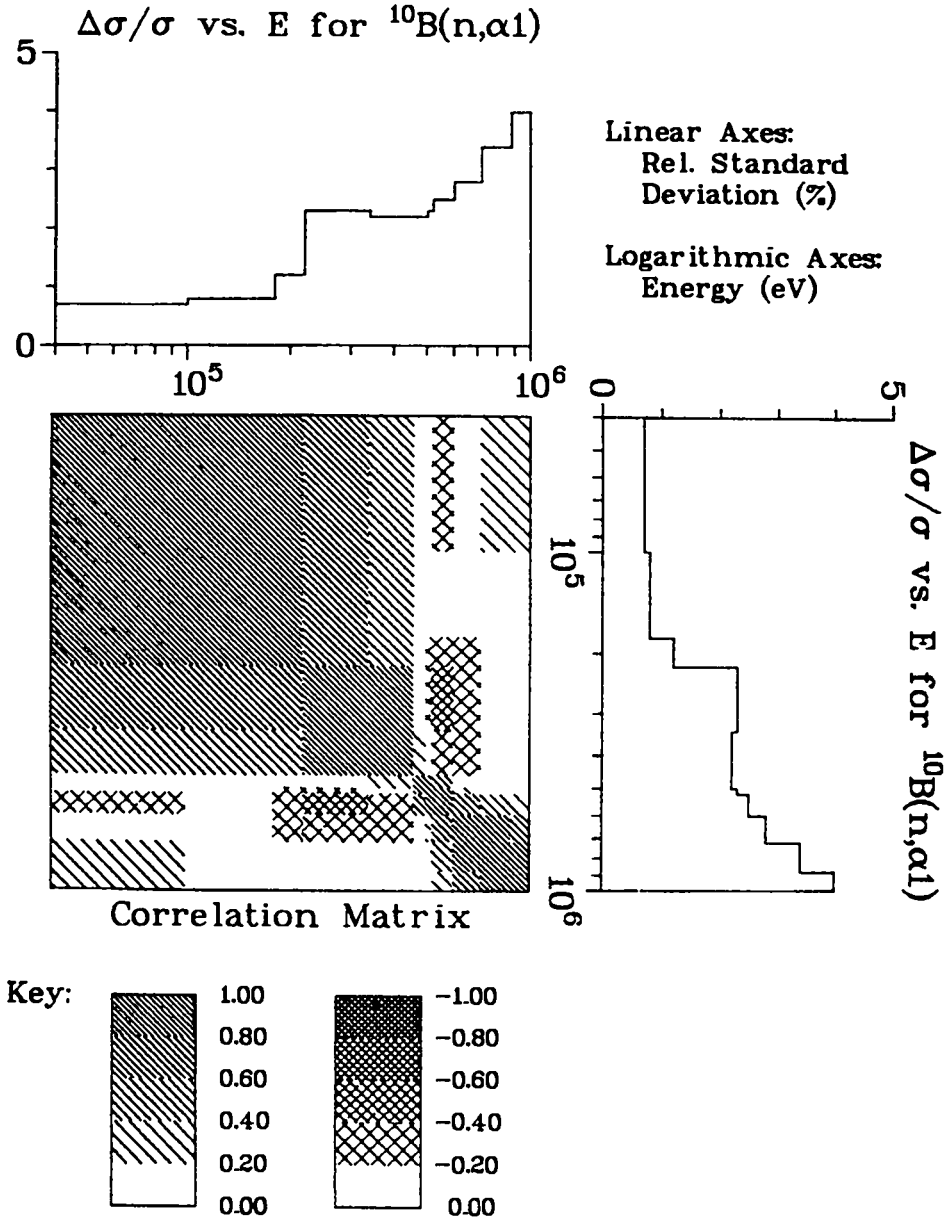

Fig. 9.
Covariances for (MAT 1305, MT 781).

III. FISSION PRODUCTS AND ACTINIDES: YIELDS, DECAY DATA, DEPLETION, AND BUILDUP

A. Neutron Production from Actinide Decay in Oxide Fuels [W. B. Wilson, R. T. Perry (U. of Wisc.), T. R. England, R. J. LaBauve, M. E. Battat, and N. L. Whittemore]

A total of 144 actinide nuclides that may be produced in reactor fuel have been described previously.[30] Of these, 60 are described with decay data in ENDF/B-V.[31] Decay data have been accumulated from available sources to describe all remaining actinides,[32] resulting in a near-complete collection of actinide data.

Neutron production in oxide fuels associated with actinide decay results from spontaneous fission (SF), delayed neutron emission, and (α,n) reactions of decay alpha particles with ^{17}O and ^{18}O. Forty of the 144 actinides have been identified as nuclides decaying at least partly by spontaneous fission. The SF neutron production of these nuclides, listed in Table IV, are given as the number of SF neutrons per decay of any kind; this is equal to the product of the SF branching fraction and $\nu(SF)$--the total number of neutrons emitted per SF decay. In turn, $\nu(SF)$ equals the sum of the $\nu_p(SF)$ (prompt) and $\nu_d(SF)$ (delayed) contributions. The branching fractions listed in Table IV were taken from ENDF/B-V or Refs. 33 and 34. Values of $\nu_p(SF)$ were taken from Ref. 26 or from the linear approximation to that data as shown in Fig. 10. The minor $\nu_d(SF)$ contributions were generally taken as 0.01.

Of the 144 actinides only ^{210}Tl decays in part by delayed neutron emission. Neutron emission is actually associated with the decay of short-lived levels of ^{210}Pb formed by the β^- decay of ^{210}Tl.[34]

The energy dependent neutron production functions $P(E_\alpha)$ for decay alphas of energy E_α have recently been calculated for four oxide fuels.[35,36] The alpha decay spectra of 89 of the actinides identified as alpha emitters have been accumulated and combined with the neutron production function for irradiated UO_2 fuel to produce (α,n) neutron production values.

The neutron production contribuitons and total values are given in Table V in units of "neutrons per decay of any kind." The half-life and total decay energy of each actinide nuclide are also listed. The results of these calculations were recently presented,[37] and a report describing the details of the work is now in preparation.

TABLE IV

SPONTANEOUS FISSION NEUTRON PRODUCTION BY ACTINIDE NUCLIDES

NUCLIDE	NU-BAR VALUES PROMPT	DELAYED	TOTAL	SPONTANEOUS FISSION BRANCHING	NEUTRONS PER NUCLIDE DECAY
90-TH-230	2.13	.01	2.14	5.330-13 C	1.14 -12
91-PA-231	1.92	.01	1.93	2.980-12 C	5.75 -12
90-TH-232	2.130±.200 D	.01	2.14	1.410-11 C	3.02 -11
92- U-232	1.70	.01	1.71	9.000-13 A	1.54 -12
92- U-233	1.75	.01	1.76	1.300-12 A	2.29 -12
92- U-234	1.80	.01	1.81	1.200-11 A	2.17 -11
92- U-235	1.85	.01	1.86	2.011-09 C	3.74 -09
92- U-236	1.900±.050 D	.01	1.91	1.200-09 A	2.29 -09
94-PU-236	2.120±.130 D	.01	2.13	8.100-10 A	1.73 -09
93-NP-237	2.04	.01	2.05	2.140-12 C	4.39 -12
92- U-238	2.000±.030 D	.01	2.01	5.450-07 A	1.095-06
94-PU-238	2.210±.070 D	.01	2.22	1.840-09 A	4.08 -09
94-PU-239	2.15	.01	2.16	4.400-12 A	9.37 -12
94-PU-240	2.151±.006 D	.01	2.16	5.000-08 A	1.08 -07
96-CM-240	2.38	.01	2.39	3.860-08 C	9.23 -08
95-AM-241	2.26	.01	2.27	4.100-12 A	9.31 -12
94-PU-242	2.141±.009 D	.01	2.15	5.500-06 A	1.18 -05
95-AM-242M	2.33	.01	2.34	1.600-10 A	3.74 -10
96-CM-242	2.510±.060 D	.01	2.52	6.800-08 A	1.71 -07
95-AM-243	2.41	.01	2.42	2.200-10 A	5.32 -10
94-PU-244	2.290±.190 D	.01	2.30	1.250-03 A	2.88 -03
96-CM-244	2.681±.011 D	.01	2.69	1.347-06 A	3.62 -06
96-CM-246	3.170±.220 D	.01	3.18	2.614-04 A	8.31 -04
96-CM-248	3.100±.090 D	.01	3.11	8.260-02 A	2.569-01
98-CF-248	3.33	.01	3.34	2.850-05 C	9.52 -05
97-BK-249	3.590±.160 D	.01	3.60	4.600-10 A	1.66 -09
98-CF-249	3.400±.400 D	.01	3.41	5.020-09 A	1.71 -08
96-CM-250	3.300±.080 D	.01	3.31	7.000-01 B	2.32 +00
98-CF-250	3.520±.090 D	.01	3.53	7.700-04 A	2.72 -03
98-CF-252	3.756±.012 D	.009 D	3.765±.010 D	3.092-02 A	1.164-01
99-ES-253	3.92	.01	3.93	8.700-08 A	3.42 -07
98-CF-254	3.890±.050 D	.01	3.90	9.969-01 C	3.888+00
99-ES-254	3.94	.01	3.95	3.020-08 C	1.19 -07
99-ES-254M	3.94	.01	3.95	4.500-08 C	1.78 -07
100-FM-254	3.980±.140 D	.01	3.99	5.900-04 C	2.35 -03
99-ES-255	3.96	.01	3.97	4.000-05 C	1.59 -04
100-FM-255	3.99	.01	4.00	2.290-07 C	9.16 -07
100-FM-256	4.00	.01	4.01	9.190-01 C	3.69 +00
100-FM-257	4.010±.130 D	.01	4.02	2.100-03 C	8.44 -03
100-FM-258	4.02	.01	4.03	1.000+00 C	4.03 +00

A=ENDF/B-V
B=A.TOBIAS, U.K., PRIVATE COMMUNICATION
C=TABLE OF ISOTOPES, SEVENTH EDITION
D=MANERO AND KONSHIN, ATOMIC ENERGY REV. 10,637-756(1972)
PROMPT NU-BAR VALUES GIVEN WITHOUT REFERENCE HAVE BEEN ESTIMATED FROM THE VALUES OF REF D. DELAYED NU-BAR VALUES GIVEN WITHOUT REFERENCE HAVE BEEN ARBITRARILY ASSUMED.

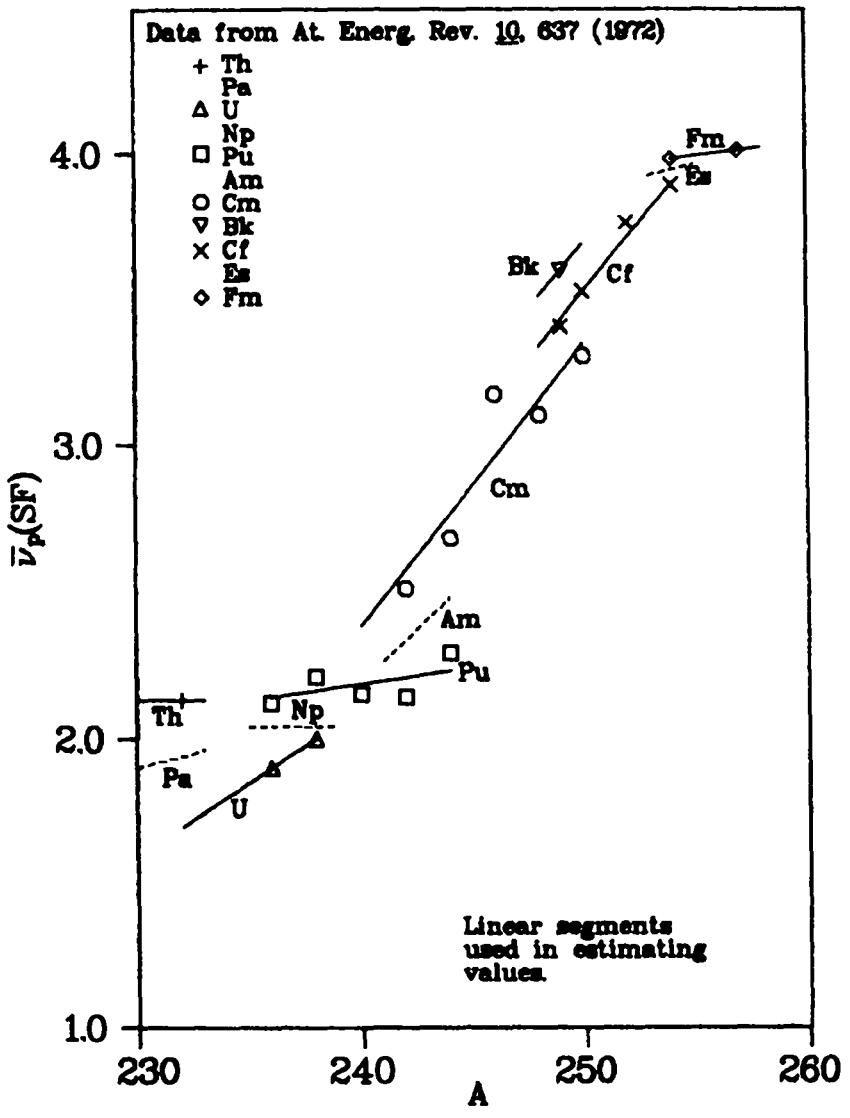

Fig. 10.
Values of $\bar{\nu}_p$(sf).

TABLE V

PRELIMINARY ACTINIDE NUCLIDE DECAY PROPERTIES

NUCLIDE	HALF-LIFE (SECONDS)	DECAY ENERGY (MEV)	DE-CAY REF	◆◆◆◆NEUTRONS PER DECAY◆◆◆◆ ALPHA,N IN UO2	SPONT. FISSION	TOTAL
80-HG-206	4.89000+2	0.5274	C	0.	0.	0.
81-TL-206	2.50980+2	0.5402	C	0.	0.	0.
82-PB-206	STABLE	0.	-	0.	0.	0.
81-TL-207	2.87400+2	0.5194	C	0.	0.	0.
82-PB-207	STABLE	0.	-	0.	0.	0.
81-TL-208	1.84200+2	3.9702	A	0.	0.	0.
82-PB-208	STABLE	0.	-	0.	0.	0.
81-TL-209	1.32000+2	2.8315	C	0.	0.	0.
82-PB-209	1.17108+4	0.2234	C	0.	0.	0.
83-BI-209	6.3115+25	0.	D	0.	0.	0.
81-TL-210	7.80000+1	4.2765	C	0.	0.	7.00 -05◆
82-PB-210	7.02472+8	0.0441	C	5.68 -17	0.	5.68 -17
83-BI-210	4.33123+5	0.3899	C	1.56 -14	0.	1.16 -14
84-PO-210	1.19557+7	5.4076	C	1.87 -08	0.	1.87 -08
82-PB-211	2.16600+3	0.5353	C	0.	0.	0.
83-BI-211	1.29000+2	6.7881	C	3.88 -08	0.	3.88 -08
84-PO-211	0.5160000	7.5942	C	5.64 -08	0.	5.64 -08
82-PB-212	3.83040+4	0.3180	A	0.	0.	0.
83-BI-212	3.63600+3	2.9030	C	1.076-08	0.	1.076-08
84-PO-212	2.96000-7	8.9536	C	8.94 -08	0.	8.94 -08
83-BI-213	2.73540+3	0.7172	C	5.85 -10	0.	5.85 -10
84-PO-213	4.20000-6	8.5360	C	7.86 -08	0.	7.86 -08
82-PB-214	1.60800+3	0.5389	C	0.	0.	0.
83-BI-214	1.18200+3	2.1923	C	4.39 -12	0.	4.39 -12
84-PO-214	1.63700-4	7.8337	C	6.19 -08	0.	6.19 -08
83-BI-215	4.44000+2	0.8445	C	0.	0.	0.
84-PO-215	1.77800-3	7.5265	C	5.52 -08	0.	5.52 -08
85-AT-215	1.00000-4	8.1780	C	6.98 -08	0.	6.98 -08
84-PO-216	0.1500000	6.9064	A	4.28 -08	0.	4.28 -08
85-AT-217	0.0323000	7.2004	C	4.85 -08	0.	4.85 -08
86-RN-217	5.40000-4	7.8880	C	6.32 -08	0.	6.32 -08
84-PO-218	1.83000+2	6.1149	C	2.909-08	0.	2.909-08
85-AT-218	1.7500000	6.8830	C	4.14 -08	0.	4.14 -08
86-RN-218	0.0350000	7.2664	C	4.99 -08	0.	4.99 -08
85-AT-219	5.40000+1	6.2165	C	3.26 -08	0.	3.26 -08
86-RN-219	3.9600000	6.9463	C	4.25 -08	0.	4.25 -08
86-RN-220	5.56000+1	6.4048	A	3.39 -08	0.	3.39 -08
87-FR-221	2.88000+2	6.4580	C	3.45 -08	0.	3.45 -08
86-RN-222	3.30351+5	5.5905	C	2.129-08	0.	2.129-08
87-FR-222	8.64000+2	0.7450	C	2.45 -11	0.	2.45 -11
88-RA-222	3.80000+1	6.6760	C	3.846-08	0.	3.846-08
87-FR-223	1.30800+3	0.4559	C	7.65 -13	0.	7.65 -13
88-RA-223	9.87949+5	------	C	2.39 -08	0.	2.39 -08
88-RA-224	3.16224+5	5.7903	A	2.40 -08	0.	2.40 -08
88-RA-225	1.27872+6	0.1433	C	0.	0.	0.
89-AC-225	8.64000+5	5.9354	C	2.57 -08	0.	2.57 -08
88-RA-226	5.0461+10	4.8708	C	1.304-08	0.	1.304-08
89-AC-226	1.04400+5	0.4099	C	1.24 -12	0.	1.24 -12

TABLE V (Continued)

NUCLIDE	HALF-LIFE (SECONDS)	DECAY ENERGY (MEV)	DE-CAY REF	◆◆◆◆NEUTRONS PER DECAY◆◆◆◆ ALPHA,N IN UO2	SPONT. FISSION	TOTAL
90-TH-226	1.85400+3	6.4517	C	3.42 -08	0.	3.42 -08
89-AC-227	6.87097+8	0.0878	C	2.01 -10	0.	2.01 -10
90-TH-227	1.61720+6	6.1466	C	2.72 -08	0.	2.72 -08
88-RA-228	1.82087+8	0.0146	C	0.	0.	0.
89-AC-228	2.20680+4	1.3696	C	0.	0.	0.
90-TH-228	6.03725+7	5.5176	A	2.004-08	0.	2.004-08
90-TH-229	2.3163+11	5.1686	C	1.391-08	0.	1.391-08
90-TH-230	2.4299+12	4.7609	A	1.207-08	1.14 -12	1.21 -08
91-PA-230	1.52928+6	0.6577	C	6.03 -13	0.	6.03 -13
92- U-230	1.79712+6	5.9928	C	2.69 -08	0.	2.69 -08
90-TH-231	9.18720+4	0.1537	A	0.	0.	0.
91-PA-231	1.0338+12	5.0601	A	1.478-08	5.75 -12	1.48 -08
92- U-231	3.62880+5	0.1017	C	1.14 -12	0.	1.14 -12
90-TH-232	4.4337+17	4.0882	A	5.52 -09	3.02 -11	5.55 -09
91-PA-232	1.13184+5	1.098	A	0.	0.	0.
92- U-232	2.26263+9	5.4145	A	1.871-08	1.54 -12	1.87 -08
90-TH-233	1.33800+3	0.4422	A	0.	0.	0.
91-PA-233	2.33280+6	0.4080	A	0.	0.	0.
92- U-233	5.0232+12	4.8978	A	1.336-08	2.29 -12	1.34 -08
90-TH-234	2.08233+6	0.1473	C	0.	0.	0.
91-PA-234	2.43000+4	2.2453	C	0.	0.	0.
91-PA-234M	7.05000+1	0.8141	C	0.	0.	0.
92- U-234	7.7188+12	4.8685	A	1.299-08	2.17 -11	1.301-08
90-TH-235	4.14000+2	------	C	0.	0.	0.
91-PA-235	1.45200+3	------	C	0.	0.	0.
92- U-235	2.2210+16	4.6651	A	8.89 -09	3.74 -09	1.26 -08◆
90- U-235M	1.48080+3	0.0001	C	0.	0.	0.
93-NP-235	3.42230+7	0.0810	C	2.44 -13	0.	2.44 -13
94-PU-235	1.53600+3	5.8675	C	3.48 -12	0.	3.48 -12
92- U-236	7.3890+14	4.5809	A	9.89 -09	2.29 -09	1.218-08
93-NP-236	3.6290+12	0.3390	A	0.	0.	0.
93-NP-236M	8.10000+4	0.1353	A	0.	0.	0.
94-PU-236	8.99688+7	5.8634	A	2.517-08	1.73 -09	2.69 -08
92- U-237	5.83200+5	0.3103	A	0.	0.	0.
93-NP-237	6.7532+13	4.9470	A	1.303-08	4.39 -12	1.303-08
94-PU-237	3.94243+6	0.0628	A	6.72 -13	0.	6.72 -13
92- U-238	1.4100+17	4.2755	A	6.64 -09	1.095-06	1.102-06
93-NP-238	1.82908+5	0.7916	A	0.	0.	0.
94-PU-238	2.76912+9	5.5871	A	2.124-08	4.08 -09	2.532-08
92- U-239	1.41000+3	0.4650	A	0.	0.	0.
93-NP-239	2.03385+5	0.4180	A	0.	0.	0.
94-PU-239	7.6084+11	5.2396	A	1.664-08	9.37 -12	1.665-08
92- U-240	5.07600+4	0.1755	C	0.	0.	0.
93-NP-240	4.02000+3	1.5755	C	0.	0.	0.
93-NP-240M	4.50000+2	1.0407	C	0.	0.	0.
94-PU-240	2.0670+11	5.3274	A	1.676-08	1.08 -07	1.25 -07
95-AM-240	1.82880+5	1.0920	A	3.74 -14	0.	3.74 -14
96-CM-240	2.31552+6	6.3844	C	3.37 -08	9.23 -08	1.26 -07

TABLE V (Continued)

NUCLIDE	HALF-LIFE (SECONDS)	DECAY ENERGY (MEV)	DE-CAY REF	◆◆◆◆NEUTRONS PER DECAY◆◆◆◆ ALPHA,N IN UO2	SPONT. FISSION	TOTAL
94-PU-241	4.63886+8	0.0054	A	3.39 -13	0.	3.39 -13
95-AM-241	1.3639+10	5.6131	A	2.115-08	9.31 -12	2.116-08
96-CM-241	2.83392+6	1.1100	A	2.79 -10	0.	2.79 -10
94-PU-242	1.1875+13	4.9812	A	1.406-08	1.18 -05	1.18 -05
95-AM-242	5.76360+4	0.1944	A	0.	0.	0.
95-AM-242M	4.79665+9	0.0631	A	9.22 -11	3.74 -10	4.56 -10
96-CM-242	1.40745+7	6.2169	A	3.07 -08	1.714-07	2.02 -07
94-PU-243	1.78452+4	0.1957	A	0.	0.	0.
95-AM-243	2.3289+11	5.4224	A	1.82 -08	5.32 -10	1.87 -08
96-CM-243	8.99372+8	6.1598	A	2.62 -08	0.	2.62 -08
94-PU-244	2.5877+15	4.6510	A	1.083-08	2.875-03	2.88 -03
95-AM-244	3.63600+4	1.1177	A	0.	0.	0.
95-AM-244M	1.56000+3	0.5088	A	0.	0.	0.
96-CM-244	5.71495+8	5.9010	A	2.582-08	3.623-06	3.65 -06
94-PU-245	3.78280+4	0.8103	C	0.	0.	0.
95-AM-245	7.38000+3	0.3199	C	0.	0.	0.
96-CM-245	2.6744+11	5.5881	A	1.948-08	0.	1.95 -08
94-PU-246	9.37440+5	0.2514	C	0.	0.	0.
95-AM-246M	1.50000+3	1.4433	C	0.	0.	0.
96-CM-246	1.4926+11	5.4714	A	1.971-08	8.313-04	8.31 -04
96-CM-247	4.9229+14	5.3522	A	1.466-08	0.	1.47 -08
96-CM-248	1.0720+13	4.7270	A	1.441-08	2.569-01	2.57 -01
97-BK-248	2.84018+8	------	C	--------	--------	--------◆
97-BK-248M	8.46000+4	0.1684	C	0.	0.	0.
98-CF-248	2.88144+7	6.3613	C	3.336-08	9.519-05	9.52 -05
96-CM-249	3.84900+3	0.2932	A	0.	0.	0.
97-BK-249	2.76480+7	0.0331	A	2.906-13	1.656-09	1.66 -09
98-CF-249	1.1064+10	6.2903	A	2.646-08	1.712-08	4.36 -08
96-CM-250	3.5660+11	------	B	--------	2.32 +00	2.32 +00
97-BK-250	1.15812+4	1.1829	A	0.	0.	0.
98-CF-250	4.12764+8	6.1227	A	2.941-08	2.718-03	2.72 -03
96-CM-251	1.00800+3	0.5925	C	0.	0.	0.
97-BK-251	3.33600+3	0.4988	C	0.	0.	0.
98-CF-251	2.8338+10	6.0260	A	2.532-08	0.	2.53 -08
98-CF-252	8.32471+7	6.0317	A	2.996-08	1.164-01	1.164-01
98-CF-253	1.53878+6	0.0980	A	8.89 -11	0.	8.89 -11
99-ES-253	1.76860+6	6.7367	A	3.995-08	3.419-07	3.82 -07
98-CF-254	5.22720+6	0.0184	C	8.167-11	3.888+00	3.888+00
99-ES-254	2.38205+7	6.6172	C	3.627-08	1.193-07	1.56 -07
99-ES-254M	1.41480+5	0.7351	C	1.138-10	1.778-07	1.78 -07
100-FM-254	1.16640+4	7.2996	C	5.08 -08	2.354-03	2.35 -03
98-CF-255	6.84000+3	------	C	0.	0.	0.

TABLE V (Continued)

NUCLIDE	HALF-LIFE (SECONDS)	DECAY ENERGY (MEV)	DE-CAY REF	◆◆◆◆NEUTRONS PER DECAY◆◆◆◆ ALPHA,N IN UO2	SPONT. FISSION	TOTAL
99-ES-255	3.30912+6	0.5956	C	2.72 -09	1.59 -04	1.59 -04
100-FM-255	7.22520+4	7.2407	C	4.75 -08	9.16 -07	9.64 -07
99-ES-256	1.32000+3	0.6169	C	0.	0.	0.
100-FM-256	9.45720+3	7.0250	C	4.55 -08	3.69 +00	3.69 +00
100-FM-257	8.68320+6	6.8640	C	3.81 -08	8.44 -03	8.44 -03
100-FM-258	3.80000-4	------	C	0.	4.03 +00	4.03 +00

DECAY DATA REFERENCES
A=ENDF/B-V
B=A.TOBIAS,U.K.,PRIVATE COMMUNICATION
C=TABLE OF ISOTOPES
◆ ADDITIONAL NOTES
MISSING DATA NOTED AS ------
81-TL-210, NEUTRONS FROM DELAYED NEUTRON EMISSION FROM 82-PB-210 LEVELS PRODUCED IN BETA DECAY.
92- U-235, SPONTANEOUS FISSION BRANCHING IN ENDF/B-V IS ZERO BY OMISSION. S.F. BRANCHING(2.011-9) TAKEN FROM REFERENCE C.
97-BK-248 DECAY CHARACTERISTICS UNKNOWN.

B. Fission-Product Decay Heat: Preliminary ENDF/B-V vs. ENDF/B-IV [T. R. England, R. J. LaBauve, W. B. Wilson, N. L. Whittemore, D. C. George, and D. E. Wessol (EG&G, Idaho)]

Most of this quarter was devoted to revising the CINDER-10 data libraries to use ENDF/B-V decay and yield data. The chain structures and libraries have been greatly expanded because of the increase in known isomeric states, the use of 105 delayed neutron precursors vs. 57 in ENDF/B-IV, and the doubling of yield sets. The chain systematics have now been thoroughly tested and the data libraries completed except for incorporation of ENDF/B-V cross sections; these are still being processed by the NJOY code. However, for thermal reactors thereis little change expected in most cross sections, and the cross sections do not affect comparisons of decay heat following a fission pulse.

Figures 11-13 compare the beta, gamma, and total decay energy rates for a ^{235}U thermal fission pulse as a ratio of ENDF/B-V to -IV. While the rates following a pulse emphasize any differences in the data base, the differences are surprisingly large, especially for the gamma energy. We are now attempting to find the reasons for the larger differences by (a) identifying the major contributors from each file base and (b) comparing nuclide decay parameters with those from other compilations such as the UK data and GAMDAT78. Earlier comparisons using ENDF/B-IV decay data with ENDF/B-V yields show changes of only 1% or less; therefore, the differences in aggregate heating are most likely due to decay energy and branching fraction changes, some of which may be in error in ENDF/B-V. Note that these differences will be reduced in any realistic calculation with an extended irradiation period.

C. LASL Meeting of the CSEWG Yields and the Fission-Product and Actinide Subcommittees (T. R. England)

The joint meeting was held at the Los Alamos Scientific Laboratory on August 5, 1980. Highlights were as follows.

- There now have been 40 fission yield sets evaluated vs. 20 in ENDF/B-V and and 10 in ENDF/B-IV. Table VI shows the fissionable nuclides and incident neutron energy ranges having yield evaluations in each case. The new evaluations are not in ENDF/B format. The new evaluations obviate most criticisms of the ENDF/B yields.

- A minimum uncertaintly limit of approximately 1% was recommended for the yields, especially those labled as from fast fission. However, this is still a subject for discussion.

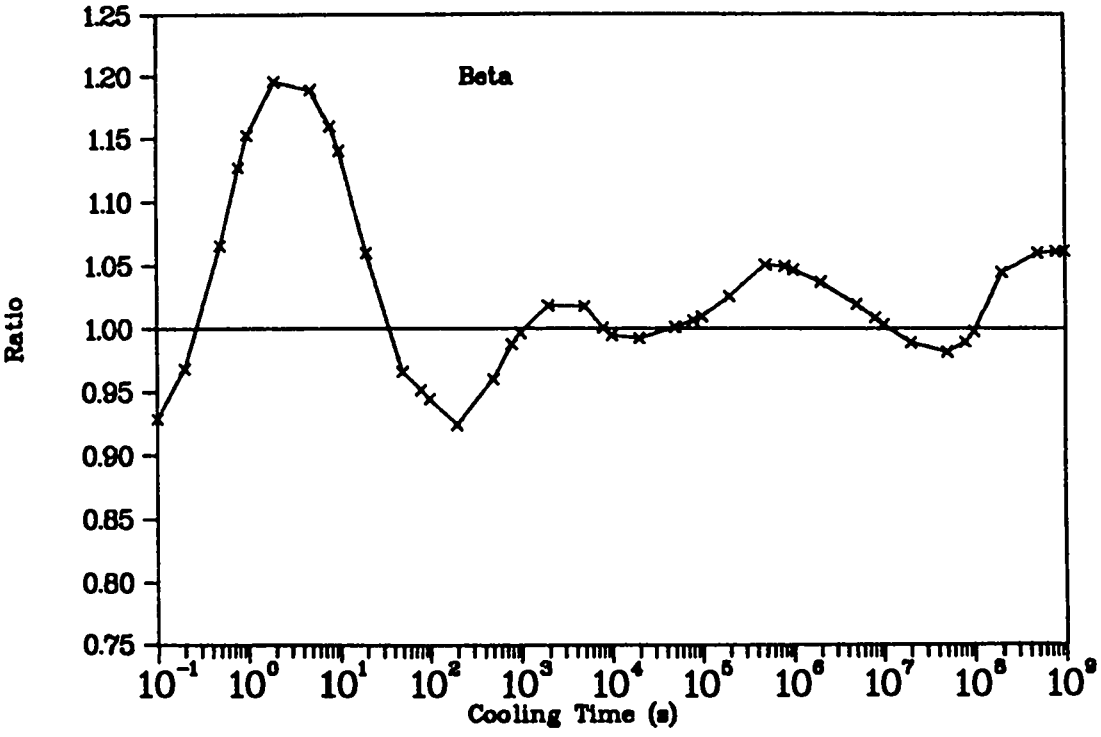

Fig. 11.
^{235}U thermal fission pulse comparison of calculated fission product decay heat; ratio of ENDF/B-V (preliminary) to ENDF/B-IV.

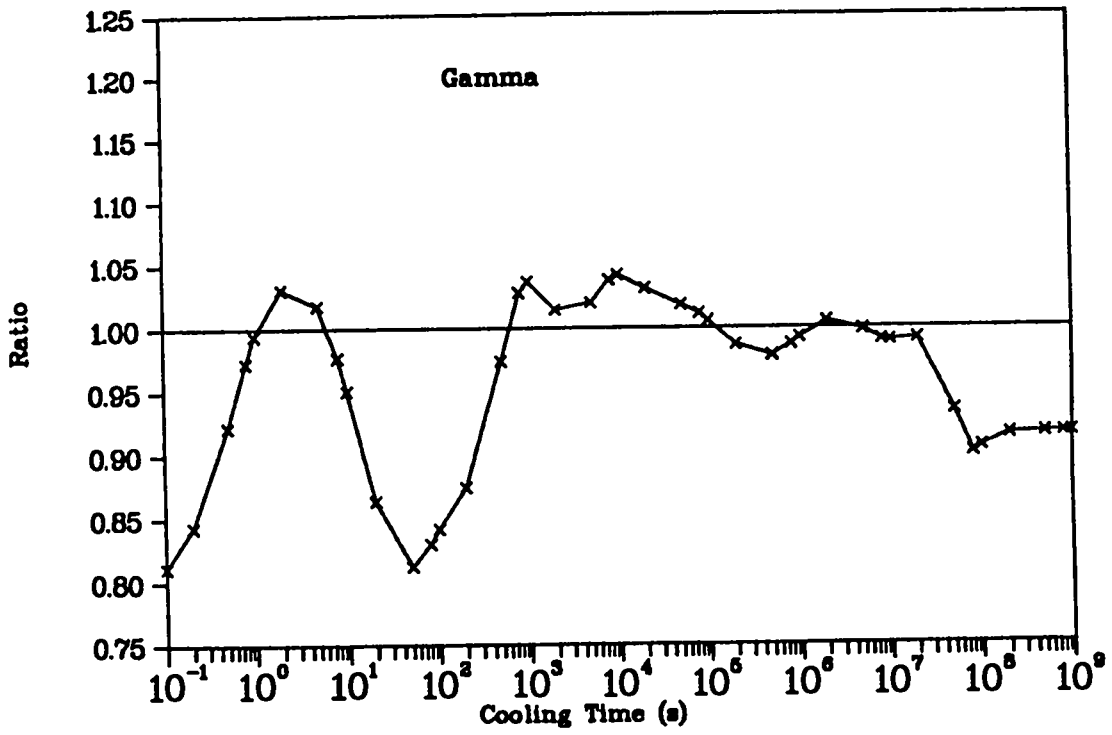

Fig. 12.
^{235}U thermal fission pulse comparison of calculated fission product decay heat; ratio of ENDF/B-V (preliminary) toENDF/B-IV.

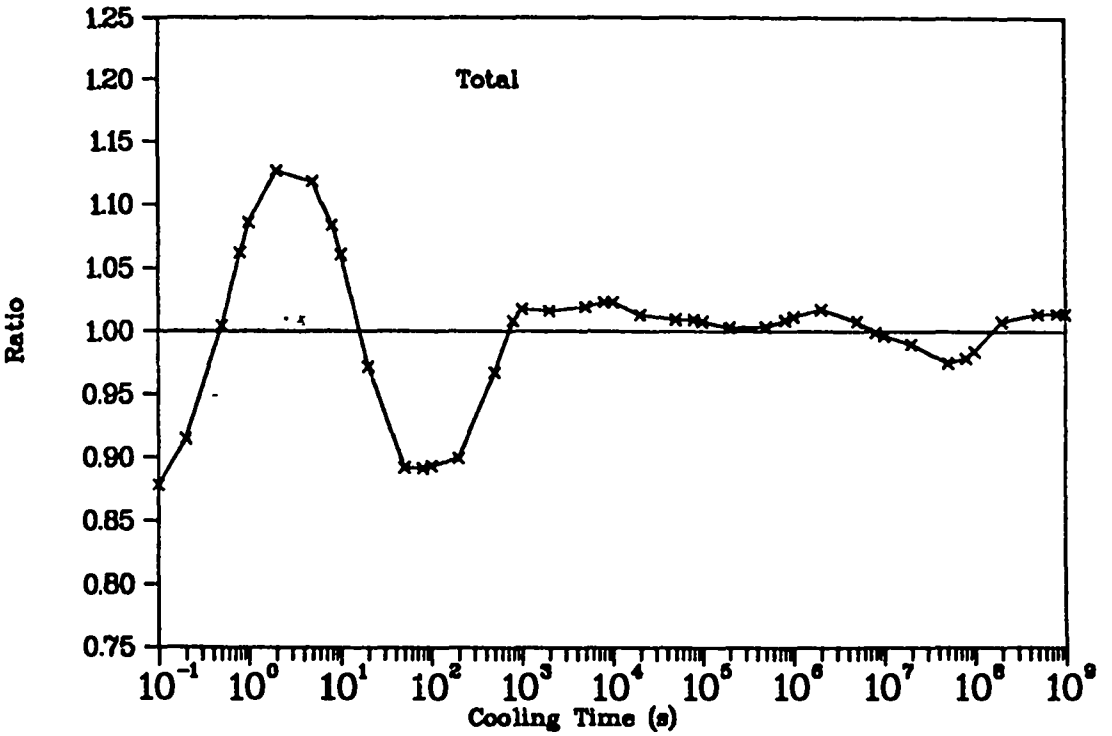

Fig. 13.
^{235}U thermal fission pulse comparison of calculated fission product decay heat; ratio of ENDF/B-V (preliminary) to ENDF/B-IV.

TABLE VI

ENDF/B YIELD SETS IN VERSIONS IV, V, AND PRELIMINARY VI[a]

Target Nuclide	Characteristic Neutron Incident Energy			
	Thermal	Fast	High (14 MeV)	Spontaneous
Th-277	6			
Th-229	6			
Th-232		4,5,6	5,6	
Pa-231		6		
U-233	4,5,6	5,6	5,6	
U-234		6	6	
U-235	4,5,6	4,5,6	4,5,6	
U-236		5,6	6	
U-237		6		
U-238		4,5,6	4,5,6	
Np-237		5,6		
Np-238		6		
Pu-238		6		
Pu-239	4,5,6	4,5,6	5,6	
Pu-240		5,6	6	
Pu-241	4,5,6	5,6		
Pu-242		5,6		
Am-241	6	6	6	
Am-242M	6			
m-243		6		
Cm-242		6		
Cm-245	6			
Cm-249	6			
Cf-251	6			
Cf-252				5,6
Es-254	6			

[a]B. F. Rider has completed a preliminary and possibly a final General Electric evaluation of the noted 40 yield sets. These have not yet been reviewed, extended as in Version V, or had inconsistencies with the decay files removed, and they are not yet available in the ENDF/B format.

- A problem for future evaluations and experimental compilations is the definition of fast as a lable for fission yields in a fast reactor spectrum. Bill Maeck from EXXON presented measurements of a few yields made in a range of fast spectra. Some nuclides show a surprisingly large energy dependence. It was recommended that future evaluations characterize the dependence where it is known and some attempt should be made to develop model estimates, depending on the degree of support for such work.

- B. Wehring's recent ^{233}U independent (direct) thermal yield measurements show that the ENDF/B-V yield uncertainties are too large by approximately 20% in about 85% of the comparisons.

- The extensive increase in evaluated cross sections was summarized. Large changes in individual cross sections for fast reactors were noted.

- The use of two fictitious fission products (lumps) to represent the aggregate fission product absorption in fast reactors was presented by B. Atefi of Brookhaven National Laboratory. He noted that accuracies of ~2% were needed in the lump approximation for use in the Fast Mixed Spectrum Reactor (FMSR) design.

- Aggregate, equilibrium delayed neutron spectra as calculated using ENDF/B-V yields, Pn values, and the individual spectra for 24 precursors (supplied by Rudstam) was presented in a passout, but not discussed.

REFERENCES

1. G. M. Hale, "Non-Orthogonal Channels in R-Matrix Theory," in "Applied Nuclear Data Research and Development April 1 - June 30, 1980," Los Alamos Scientific Laboratory report LA-8524-PR, p. 1 (1980).

2. A. M. Lane and R. G. Thomas, "R-Matrix Theory of Nuclear Reactions," Rev. Mod. Phys. 30, 257 (1958).

3. W. Tobocman, "New Coupled-Reaction-Channels Formalism for Nuclear Reactions," Phys. Rev. C11, 43 (1975).

4. C. Chandler and A. Gibson, "Two Hilbert Space Formulation of Scattering Theory," in Proc. of Mathematical Methods and Applications of Scattering Theory, Vol. 130, Lecture Notes in Physics (Springer-Verlag, NY) (1978).

5. P. G. Young, R. E. MacFarlane, and R. B. Kidman, "n + Gallium Evaluation," in "Applied Nuclear Data Research and Development Quarterly Progress Report, January 1-March 31, 1980," compiled by C. I. Baxman and P. G. Young, Los Alamos Scientific Laboratory report, p. 6, LA-8418-PR (1980).

6. V. A. Konks, personal communication via National Neutron Cross Center Center, Brookhaven National Laboratory (1964).

7. A. G. Dovbenko, V. E. Kolesov, V. P. Koroleva, and V. A. Tolstikov, Atomnaya Eergiya 26, 67 (1969).

8. G. G. Zaikin, I. A. Korzh, M. V. Pasechnic, and N. T. Skljar, UKR. Fiz. Zh. 16, 1205 (1971).

9. In collaboration with A. B. Smith, Argonne National Laboratory, and C. A. Philis, Bruyeres-le-Chatel (France).

10. J. Raynal, "Optical Model and Coupled-Channel Calculations in Nuclear Physics," International Atomic Energy Agency report IAEA-SMR-9/8 (1972)

11. C. L. Dunford, "A Unified Model for Analysis of Compound Nucleus Reactions," Atomics International report AI-AEC-12931 (July 1970).

12. P. G. Young and E. D. Arthur, "GNASH" A Preequilibrium Statistical Nuclear Model Code for Calculations of Cross Sections and Emission Spectra," Los Alamos Scientific Laboratory report LA-6947 (Nov. 1977).

13. E. D. Arthur, "Parameter Determination and Application to Nuclear Model Calculations of Neutron-Induced Reactions on Yttrium and Zirconium Isotopes," accepted for publication in Nucl. Sci. Eng. (1980).

14. E. D. Arthur and P. G. Young, "Evaluation of Neutron Cross Sections to 40 MeV for $^{54\ 56}$Fe," Proc. Symp. on Neutron Cross Sections from 10 to 50 MeV," Upton, NY (May 1980).

15. S. Joly, Bruyeres-le-Chatel, personal communication (1980).

16. A. Gilbert and A. G. W. Cameron, "A Composite Nuclear-Level Density Formula with Shell Corrections," Can. J. Phys. 43, 1446 (1965).

17. J. P. Delaroche, G. Haouat, J. Lachkar, Y. Patin, J. Sigaud, and J. Chardine, "Coherent Optical and Statistical Model Analysis of ^{182,183,184} ^{186}W Neutron Cross Sections," Proc. Int. Conf. on Nuclear Cross Sections for Technology, Knoxville, TN (1979).

18. J. Frehaut and J. Jary, "Systematique des Sections Efficaces de Reactions (n,2n) pour des Series d'Isotopes Separes," Proc. Int. Conf. on Neutron Data and Nuclear Data, Harwell, p. 1038 (1978).

19. P. T. Guenther, "The Elastic and Inelastic Scattering of Fast Neutrons from the Even Isotopes of Tungsten," U. of Illinois Ph. D. Thesis, unpublished (1977).

20. J. K. Dickens, T. A. Love, and G. L. Morgan, "Gamma-Ray Production due to Interactions with Tungsten for Incident Neutron Energies between 0.1 and 20 MeV," ORNL-4847 (1973).

21. D. Hermsdorf, A. Meister, S. Sassonoff, D. Selliger, and K. Seidel, "Absolute Differentielle Neutronenemissionsquerschnitte fur Ga, Se, Br, Zr, Nb, Cd, In, Sn, Sb, J, Ta, W, Au, Hg, Pb, and Be bei 14 MeV Einschussenergie," Kernenergie 1, 241 (1976).

22. D. G. Madland, "Prompt Fission Neutron Spectra and $\bar{\nu}_p$," invited paper in Proc. Workshop on Evaluation Methods and Procedures, Brookhaven National Laboratory, Sept. 22-25, 1980 (to be published).

23. D. G. Madland and J. R. Nix, "Calculation of Prompt Fission Neutron Spectra," in Proc. of the Int. Conf. on Nuclear Cross Sections for Technology, Knoxville, TN, October 22-26, 1979 (to be published).

24. D. G. Madland and J. R. Nix, "Calculation of Neutron Spectra and Average Neutron Multiplicities from Fission," in Proc. Int. Conf. on Nuclear Physics, Berkeley, CA, August 24-30, 1980 (to be published).

25. D. C. Hoffman and M. M. Hoffman, "Post-Fission Phenomena," Ann. Rev. Nuc. Sci. 24, 151 (1974).

26. F. Manero and V. A. Konshin, "Status of the Energy-Dependent ν-Values for the Heavy Isotopes (Z>90) from Thermal to 15 MeV and of ν-Values for Spontaneous Fission," At. Energ. Rev. 10, 637 (1972).

27. O. Ozer, Electric Power Research Institute, personal communication.

28. R. E. MacFarlane, R. J. Barrett, D. W. Muir, and R. M. Boicourt, "The NJOY Nuclear Data Processing System: User's Manual," Los Alamos Scientific Laboratory report LA-7584-M (1978).

29. "DISSPLA (Display Integrated Software System and Plotting Language): User's Manual," Integrated Software Systems Corporation, 4186 Sorrento Valley Blvd., San Diego, CA 92121.

30. W. B. Wilson, T. R. England, R. J. LaBauve, M. Battat, and N. L. Whittemore, "CINDER Actinide Decay Library Development," in "Applied Nuclear Data Research and Development January 1 - March 31, 1980," Los Alamos Scientific Laboratory report LA-8418-PR (June 1980).

31. T. R. England, W. B. Wilson, and N. L. Whittemore, "Summary of Actinide Decay Data in ENDF/B-V," in "Applied Nuclear Data Research and Development, January 1 - March 31, 1980," Los Alamos Scientific Laboratory report LA-8418-PR (June 1980).

32. M. E. Battat, W. B. Wilson, R. J. LaBauve, and T. R. England, "Actinide Decay Data," in "Applied Nuclear Data Research and Development, April 1 - June 30, 1980," Los Alamos Scientific Laboratory report LA-8524-PR (Sept. 1980).

33. A. Tobias, United Kingdom, personal communication.

34. C. M. Lederer and V. S. Shirley, Eds., Table of Isotopes, Seventh Edition (John Wiley and Sons, Inc., New York, 1978).

35. R. T. Perry and W. B. Wilson, "The (α,n) Neutron Production by Alpha Particles in PuO_2, UO_2, and ThO_2 Fuels," in "Applied Nuclear Data Research and Development, April 1 - June 30, 1980," Los Alamos Scientific Laboratory report LA-8524-PR (Sept. 1980).

36. R. T. Perry and W. B. Wilson, "Neutron Production from (α,n) Reactions in PuO_2, UO_2, and ThO_2 Fuels," to be presented at the Nov. 1980 ANS Meeting in Washington, D.C.

37. W. B. Wilson, T. R. England, R. J. LaBauve, M. E. Battat, D. E. Wessol, and R. T. Perry, "Status of CINDER and ENDF/B-V Based Libraries for Transmutation Calculations," Proc. Int. Conf. on Nuclear Waste Transmutation, Austin, TX (July 1980).

☆U.S. GOVERNMENT PRINTING OFFICE: 1980—777-022/231

Printed in the United States of America
Available from
National Technical Information Service
US Department of Commerce
5285 Port Royal Road
Springfield, VA 22161

Microfiche $3.50 (A01)

Page Range	Domestic Price	NTIS Price Code	Page Range	Domestic Price	NTIS Price Code	Page Range	Domestic Price	NTIS Price Code	Page Range	Domestic Price	NTIS Price Code
001-025	$ 5.00	A02	151-175	$11.00	A08	301-325	$17.00	A14	451-475	$23.00	A20
026-050	6.00	A03	176-200	12.00	A09	326-350	18.00	A15	476-500	24.00	A21
051-075	7.00	A04	201-225	13.00	A10	351-375	19.00	A16	501-525	25.00	A22
076-100	8.00	A05	226-250	14.00	A11	376-400	20.00	A17	526-550	26.00	A23
101-125	9.00	A06	251-275	15.00	A12	401-425	21.00	A18	551-575	27.00	A24
126-150	10.00	A07	276-300	16.00	A13	426-450	22.00	A19	576-600	28.00	A25
									601-up	†	A99

†Add $1.00 for each additional 25-page increment or portion thereof from 601 pages up.